Automatika

Journal for Control, Measurement, Electronics, Computing and Communications

ISSN: (Print) (Online) Journal homepage: www.tandfonline.com/journals/taut20

Finite-time kinematic path-following control of underactuated ASV with disturbance observer

Lina Jin, Shuanghe Yu, Guoyou Shi & Xiaohong Wang

To cite this article: Lina Jin, Shuanghe Yu, Guoyou Shi & Xiaohong Wang (2024) Finite-time kinematic path-following control of underactuated ASV with disturbance observer, Automatika, 65:1, 303-311, DOI: 10.1080/00051144.2023.2298099

To link to this article: https://doi.org/10.1080/00051144.2023.2298099

Published online: 08 Jan 2024.

AUTOMATIKA
2024, VOL. 65, NO. 1, 303–311
https://doi.org/10.1080/00051144.2023.2298099

Finite-time kinematic path-following control of underactuated ASV with disturbance observer

Lina Jin[a,b], Shuanghe Yu[c], Guoyou Shi[a] and Xiaohong Wang[b]

[a]College of Navigation, Dalian Maritime University, Dalian, People's Republic of China; [b]School of Artificial Intelligence and Software, Liaoning Petrochemical University, Fushun, People's Republic of China; [c]College of Marine Electrical Engineering, Dalian Maritime University, Dalian, People's Republic of China

ABSTRACT

Based on a line-of-sight (LOS) guidance law for a curve parametrized path, a finite-time backstepping control is proposed for the kinematic path-following of an underactuated autonomous surface vehicle (ASV). Finite-time observer is utilized to estimate the unknown external disturbances accurately. The first-order Levant differentiator is introduced into the finite-time filter technique, such that the output of filter can not only approximate the derivative of the virtual control, but also avoid the singularity problem of real heading control. The integral terminal sliding mode is employed to improve the tracking performance and converging rate in the surging velocity control. By virtue of Lyapunov function, all the signals in the closed-loop system can be guaranteed uniformly ultimate boundedness, and accurate path-following task can be fulfilled in finite time. The simulation results and comparative analysis validate the effectiveness and robustness of the proposed control approach.

ARTICLE HISTORY
Received 1 May 2021
Accepted 23 November 2023

KEYWORDS
Disturbance observer; finite-time control; kinematic path-following; curve parametrized path; underactuated ASV

1. Introduction

Due to its wide application in different fields, the control problem of autonomous surface vehicle (ASV) has attracted great attention from scholars in recent years, including point stabilization, trajectory tracking, path-following, platoon formation, etc. [1–5]. The goal of path-following is to design a control scheme to drive the ASV to track a predefined geometric reference [6]. The scheme usually consists of guidance and control subsystems, and a look-ahead-based line-of-sight (LOS) law is an effective way to provide a desired course such that an effective control law can be designed to drive ASV to the desired path [7,8]. Because of the complex model nonlinearity, unknown hydrodynamic coefficients, external disturbances and under-actuation characteristics, the design of ASV motion controller is a difficult task [9].

A variety of advanced control methods have been developed for path-following control of ASV, such as cascade control [10], adaptive backstepping control [11,12], sliding mode control [13–15], fuzzy neural network control [16–18]. There is a common feature that the control methods are applied to fully actuated ASV, which has great limitations in practical application. The underactuated characteristics of the ASV means that the dimension of the control input is less than the number of degrees of freedom, leading to the second-order nonholonomic constraint condition that the acceleration is not integrable, which makes it difficult for ASV to track the expected path [19].

Nonparametric uncertainties and environmental disturbances are the challenges of strongly coupled nonlinear multivariable underactuated ASV systems [20]. With a surge-guided LOS, a fuzzy disturbance observer-based path-following control scheme is proposed for an underactuated ASV [21]. A L1 adaptive backstepping control scheme is proposed for the path-following of an underactuated ASV, considering both the robustness and fast adaptation [22]. A prefilter adaptive backstepping controller is designed for an underactuated ASV to track the predefined path with a better performance of the waypoint-based navigation [23]. With the time delay control method and extended state observer technique compensating for the effects of time-varying ocean currents, a backstepping control is used to realize compound LOS guided path-following of an underactuated ASV [24]. The common point in the above works is the closed-loop systems are asymptotically stable.

Compared to asymptotic stability, finite-time stability has faster convergence rate, stronger disturbance rejection and higher steady precision [25]. A finite-time command filtered backstepping approach is adopted for the path-following of an underactuated ASV with parametric uncertainties and unknown disturbances [26]. A finite-time path-following controller is established via backstepping technique, and the unknown disturbances are estimated by an adaptive fuzzy system [27]. An adaptive vector-backstepping control is designed for

CONTACT Shuanghe Yu shuanghe@dlmu.edu.cn College of Marine Electrical Engineering, Dalian Maritime University, Dalian, China, 116026

an underactuated ASV with single unknown parameter for finite-time convergence of position tracking errors [28]. However, all the above results can only give the finite-time convergence to a neighbourhood around zero. The standard first-order of sliding modes provide for finite-time convergence with respect to internal and external disturbances, meanwhile the higher-order sliding modes preserve the main properties of the standard sliding mode [29]. A continuous finite-time control scheme using the form of terminal sliding modes is proposed [30]. A sliding mode control method with the variable-parameter double-power reaching law is proposed to weaken the chattering phenomenon [31].

Motivated by the afore-mentioned analyses, an LOS based finite-time kinematic path-following controller for an underactuated ASV subjects to ocean currents is proposed in this paper, and the main contribution is that the finite-time convergence to precise zero of path-following error is achieved by the integrated use of LOS guidance law, finite-time disturbance observer, first-order Levant differentiator, filter error compensator and terminal sliding mode [29–31], at the same time, the differentiation explosion and singularity problems of fractional-power virtual control are avoided.

The remainder of this paper is organized as follows. The ASV mode and problem formulation are presented in Section 2. The disturbance observer design for the underactuated ASV is presented in Section 3. Guided LOS motion control of ASVs using finite-time backstepping technique and the stability analysis of the closed-loop system are provided in Section 4. The simulation results are presented in Section 5.

2. Problem formulation

In this section, the mathematical model of an underactuated ASV, the definition of kinematic path-following error is firstly given, then the control objective is formulated.

2.1. Underactuated ASV model

Neglecting the motions in heave, roll, and pitch, the three-degree-of-freedom kinematic and dynamic model of the ASV can be respectively described as:

$$\begin{cases} \dot{x} = u\cos\psi - v\sin\psi \\ \dot{y} = u\sin\psi + v\cos\psi \\ \dot{\psi} = r \end{cases} \tag{1}$$

$$\begin{cases} m_{11}\dot{u} = f_u(u,v,r) + \tau_u + d_u \\ m_{22}\dot{v} = f_v(u,v,r) + d_v \\ m_{33}\dot{r} = f_r(u,v,r) + \tau_r + d_r \end{cases} \tag{2}$$

where x, y, ψ represent position and the heading angle of the underactuated ASV in the earth-fixed frame, u, v, r are the velocities (surge, sway, yaw) of the ASV in the body-fixed frame, m_{11}, m_{22}, m_{33} denote the combined terms of mass and inertia parameters, d_{11}, d_{22}, d_{33} denote hydrodynamic damping and friction terms, τ_u and τ_r are the control inputs provided by the thruster, d_u, d_v, d_r represent the bounded external disturbances induced by waves and wind, and

$$\begin{cases} f_u(u,v,r) = m_{22}vr - d_{11}u \\ f_v(u,v,r) = -m_{11}ur - d_{22}v \\ f_r(u,v,r) = (m_{11} - m_{22})uv - d_{33}r \end{cases}$$

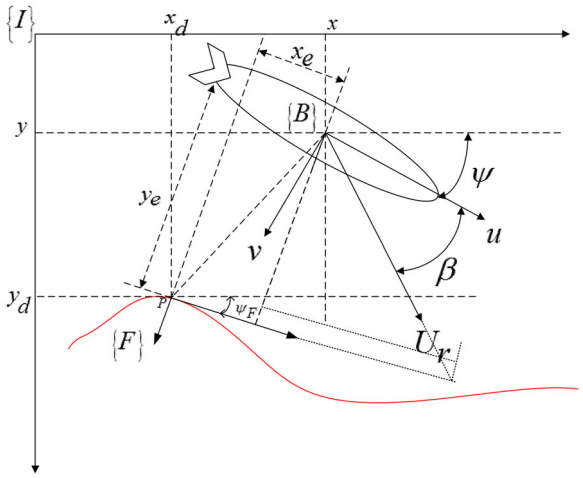

Figure 1. Path-following in the horizontal plane.

Assumption 2.1: For the system (2), there exist positive constants D_u, D_v, D_r, such that d_u, d_v, d_r satisfy the following conditions $|\dot{d}_u| \le D_u$, $|\dot{d}_v| \le D_v$, $|\dot{d}_r| \le D_r$.

2.2. Kinematic path-following error

The path-following problem in the horizontal plane is illustrated in Figure 1, where $\{I\}$, $\{B\}$ and $\{F\}$ represent the earth-fixed frame, body-fixed frame and the Serret-Frenet frame, respectively.

The following variables are defined as:

$$\begin{cases} \psi_F = \arctan\left(\dfrac{\dot{y}_d(\theta)}{\dot{x}_d(\theta)}\right) \\ \beta = \arctan\left(\dfrac{v}{u}\right) \\ U_r = \sqrt{u^2 + v^2} \end{cases} \tag{3}$$

where $[x_d, y_d]^T$ is the desired position vector of the moving virtual target on the curve parametrized path in the Serret-Frenet frame, and θ is the path parameter. Then, the path-following error vector in the Serret-Frenet frame is

$$\begin{bmatrix} x_e \\ y_e \end{bmatrix} = \begin{bmatrix} \cos\psi_F & \sin\psi_F \\ -\sin\psi_F & \cos\psi_F \end{bmatrix} \begin{bmatrix} x - x_d \\ y - y_d \end{bmatrix} \tag{4}$$

Differentiating x_e and y_e yield.

$$\dot{x}_e = u\cos\psi - v\sin\psi\cos\psi_F + u\sin\psi + v\cos\psi\sin\psi_F$$

$$
\begin{aligned}
&+[-\sin\psi_F(x-x_d)+\cos\psi_F(y-y_d)]\dot{\psi}_F\\
&-(u_{tar}\sin^2\psi_F+u_{tar}\cos^2\psi_F)\\
\dot{y}_e=&-u\cos\psi-v\sin\psi\sin\psi_F+u\sin\psi\\
&+v\cos\psi\cos\psi_F\\
&-[\cos\psi_F(x-x_d)+\sin\psi_F(y-y_d)]\dot{\psi}_F\\
&+(u_{tar}\sin\psi_F\cos\psi_F-u_{tar}\sin\psi_F\cos\psi_F),
\end{aligned}
$$

where $u_{tar}=\dot{\theta}\sqrt{\dot{x}_d^2(\theta)+\dot{y}_d^2(\theta)}$ is the velocity of the virtual target along the desired path, which can be further simplified as

$$
\begin{cases}
\dot{x}_e=u\cos(\psi-\psi_F)-u\sin(\psi-\psi_F)\tan\beta\\
\quad+\dot{\psi}_F y_e-u_{tar}\\
\dot{y}_e=u\sin(\psi-\psi_F)+u\cos(\psi-\psi_F)\tan\beta\\
\quad-\dot{\psi}_F x_e
\end{cases}
\tag{5}
$$

2.3. Control objective

The objective of this paper is to design an appropriate controller to adjust the motion path of the ASV on the horizontal surface, so that it can quickly follow the desired path, which can be realized by two subsystems:

Geometric objective: Given a desired path and the following error dynamics, the desired heading angle ψ_d and desired angular velocity r_d can be given by a LOS guidance scheme, and then u_{tar} can be designed to make the ASV converge to and move along the desired path.

Dynamic objective: Based on the underactuated ASV model, the longitudinal and heading control laws τ_u and τ_r can be designed such that the speed tracking errors $u-u_d$ and $r-r_d$ converge to an arbitrarily small neighbourhood around zero in finite time.

3. Nonlinear disturbance observer design

In order to dealing with the external disturbances suffered by an ASV in (2), a finite-time disturbance observer is constructed in this section. The following lemma is given before the design.

Lemma 3.1 ([28]): *For the second order systems*

$$
\begin{cases}
\dot{x}_1=-\mu_1 sig^{\frac{1}{2}}(x_1)+x_2\\
\dot{x}_2=-\mu_2 sgn(x_1)+L
\end{cases}
\tag{6}
$$

there exists a constant L_M satisfying$|L|\ \langle L_M,\mu_1\rangle\ 1.1L_M$, $\mu_2>1.5L_M$, the dynamic system is finite-time stable, where $sig^{\alpha}(x_1)=|x_1|^{\alpha}sgn(x_1), x_1\epsilon R,\alpha\epsilon(0,1)$,

$$
sgn(x_1)=\begin{cases}-1, & if\ x_1<0\\ [-1,1], & if\ x_1=0\\ 1, & if\ x_1>0\end{cases}
$$

The ASV dynamics are described as follows

$$
M\dot{\upsilon}=f(\upsilon)+\tau+d \tag{7}
$$

where$M=diag(m_{11},m_{22},m_{33})$, $\upsilon=[u,v,r]^T$, $f(\upsilon)=[f_u,f_v,f_r]^T$, $\tau=[\tau_u,0,\tau_r]^T$, $d=[d_u,d_v,d_r]^T$.

Theorem 3.1: *Suppose that Assumption 2.1 holds, there exists D, such that $\dot{d}\le D$, $D=[D_u,D_v,D_r]^T$, and define the errors $\Pi=\begin{bmatrix}\Pi_u & \Pi_v & \Pi_r\end{bmatrix}^T$ as*

$$
\Pi=M\upsilon-M\mathrm{X} \tag{8}
$$

$$
\dot{\mathrm{X}}\triangleq M^{-1}\left[f(\upsilon)+\tau+\mu_1 sig^{\frac{1}{2}}(\Pi)+\int_0^t\mu_2 sign(\Pi)dt\right] \tag{9}
$$

where μ_1, μ_2 are constants, then the estimated disturbance is

$$
\hat{d}=\int_0^t\mu_2 sign(\Pi)dt \tag{10}
$$

***Proof*:** Taking the derivative of (8) yields

$$
\dot{\Pi}=M\dot{\upsilon}-M\dot{\mathrm{X}}
$$

Substituting equation (7) into the above equation yields

$$
\dot{\Pi}=M\dot{\upsilon}-M\dot{\mathrm{X}}=-\mu_1 sig^{\frac{1}{2}}(\Pi)-\int_0^t\mu_2 sign(\Pi)dt+d
$$

Define $\pi=-\int_0^t\mu_2 sign(\Pi)dt+d$, then.

$$
\begin{cases}
\dot{\Pi}=-\mu_1 sig^{\frac{1}{2}}(\Pi)+\pi\\
\dot{\pi}=-\mu_2 sign(\Pi)+\dot{d}
\end{cases}
\tag{11}
$$

Based on Lemma 3.1 and Assumption 2.1, the errors $\Pi=0,\pi=0$ are achieved in finite time t_d. When $t>t_d$, $-\int_0^t\mu_2 sign(\Pi)dt+d=d-\hat{d}=0$. Then the observer can accurately estimate the disturbance in finite time. ■

4. Controller design

Based on the observed disturbance (10), the kinematic control, heading and velocity control are respectively designed in the following, and the curve parametrized path is exactly followed in finite time.

4.1. Kinematic control design

LOS is a classical guidance algorithm as well as a geometric method. The main idea of LOS guidance is to mimic the action of the helmsman, which the desired heading angle is obtained through the actual position of the ASV looking ahead to the desired position, and then a control law is utilized to steer the vehicle head for LOS angle, finally converge to the desired path. LOS Guidance law is independent of the ASV controller design,

the desired heading course of ASV is dependent on its current position and the given path.

Theorem 4.1: *If a LOS guidance law is employed as*

$$\psi_d = \psi_F - \arctan\left(\tan\beta + \frac{y_e}{\Delta}\right) \tag{12}$$

where $\Delta > 0$ is the forward view distance parameter, $\psi - \psi_F \approx \psi_d - \psi_F \in (-\pi/2, \pi/2)$ and the velocity of the virtual target along the curved parametrized path is designed as

$$u_{tar} = k_0 x_e + U_r \cos(\psi - \psi_F + \beta) \tag{13}$$

where $k_0 > 0$, then the path can be followed asymptotically.

Proof: Since.

$$\begin{aligned} \sin(\psi - \psi_F) &= -\frac{\Delta\tan\beta + y_e}{\sqrt{\Delta^2 + (\Delta\tan\beta + y_e)^2}} \\ \cos(\psi - \psi_F) &= \frac{\Delta}{\sqrt{\Delta^2 + (\Delta\tan\beta + y_e)^2}} \end{aligned} \tag{14}$$

Consider the Lyapunov function candidate

$$V = \frac{1}{2}(x_e^2 + y_e^2) \tag{15}$$

Differentiating (15) and utilizing (14) yield

$$\dot{V} = -k_0 {x_e}^2 - \frac{u {y_e}^2}{\sqrt{\Delta^2 + (y_e + \Delta\tan\beta)^2}}$$

where $u > u_{min} > 0$, then V is bounded, x_e and y_e are asymptotically stable. ■

4.2. Heading control design

In order to eliminate the differentiation explosion of the traditional backstepping control and singularity of finite-time control, the LOS guidance law and the finite time filter are introduced into heading control to enable the ASV reach the desired target in finite time.

Lemma 4.1 ([24]): *For the first order Levant differentiator is*

$$\begin{cases} \dot{\beta}_1 = z \\ z = -l_1|\beta_1 - \alpha|^{\frac{1}{2}} sign(\beta_1 - \alpha) + \beta_2 \\ \dot{\beta}_2 = -l_2 sign(\beta_2 - z) \end{cases} \tag{16}$$

where α is input signal, l_1 and l_2 are positive constants, the output signal β_1 and $\dot{\beta}_1$ of the command filter can be used to estimate α and $\dot{\alpha}$, i.e. $\beta_1 = \alpha$, $z = \dot{\beta}_1 = \dot{\alpha}$, in finite time by choosing appropriate parameters and without noise in α.

The filtering error $\beta_1 - \alpha$ is generally ignored in the traditional dynamic surface technique, which will inevitably affect the control accuracy. Therefore, the filtering error compensation mechanism is introduced for improving the performance of closed-loop system.

Lemma 4.2 ([25]): *Let the input noise satisfy the inequality $|\alpha - \alpha_0| \le o$. Then the following inequalities are established in finite time for some positive constants σ_1 and σ_2 depending exclusively on the parameters of the differentiator,*

$$\begin{aligned} |\beta - \alpha_0| &\le \sigma_1\kappa = \varrho_1 \\ \left|\dot{\beta}_1 - \dot{\alpha}_0\right| &\le \sigma_2\kappa^{\frac{1}{2}} = \varrho_2 \end{aligned} \tag{17}$$

where ϱ_1 and ϱ_2 are positive constants.

Lemma 4.3 ([26]): *An extended Lyapunov condition of finite-time stability can be given*

$$\dot{V}(x) + h_1 V(x) + h_2 V^{\gamma}(x) \le 0, 0 < \gamma < 1 \tag{18}$$

where the settling time can be estimated by

$$T \le \frac{1}{h_1(1-\gamma)} \ln \frac{h_1 V^{1-\gamma}(x_0) + h_2}{h_2} \tag{19}$$

Define the angle tracking errors z_1, z_2 and the tracking error compensations ϖ_1, ϖ_2 as

$$z_1 = \psi - \psi_d, z_2 = r - \beta_1 \tag{20}$$

$$\varpi_1 = z_1 - \zeta_1, \varpi_2 = z_2 - \zeta_2 \tag{21}$$

The virtual control law is defined as

$$\alpha = -k_1 z_1 + \dot{\psi}_d - s_1|\varpi_1|^{\gamma} sign(\varpi_1) \tag{22}$$

where k_1 and s_1 are positive constants, $0 < \gamma < 1$. Filtering error compensation is presented as

$$\dot{\zeta}_1 = -k_1\zeta_1 + (\beta_1 - \alpha) + \zeta_2 - \rho_1 sign(\zeta_1) \tag{23}$$

$$\dot{\zeta}_2 = -k_2\zeta_2 - \zeta_1 - \rho_2 sign(\zeta_2) \tag{24}$$

where k_2, ρ_1 and ρ_2 are positive constants.

Consider the Lyapunov function candidate

$$V_1 = \frac{1}{2} m_{33} {\varpi_1}^2 \tag{25}$$

Differentiating (25), utilizing (20)-(24), we can obtain

$$\begin{aligned} \dot{V}_1 = m_{33}\varpi_1(&\varpi_2 - k_1\varpi_1 - s_1|\varpi_1|^{\gamma} sign(\varpi_1) \\ &+ \rho_1 sign(\zeta_1)) \end{aligned} \tag{26}$$

From (2) we have

$$\begin{aligned} m_{33}\dot{\varpi}_2 = f_r + \tau_r + d_r - m_{33}\dot{\beta}_1 + k_2 m_{33}\zeta_2 \\ + m_{33}\zeta_1 + m_{33}\rho_2 sign(\zeta_2) \end{aligned} \tag{27}$$

where $f_r = f_r(u, v, r) = (m_{11} - m_{22})uv - d_{33}r$.

The heading tracking control law is constructed as follows:

$$\tau_r = -(m_{11} - m_{22})uv + d_{33}r - \hat{d}_r + m_{33}\dot{\beta}_1 - m_{33}z_1 - m_{33}k_2z_2 - m_{33}s_2|\varpi_2|^{\gamma}sign(\varpi_2) \tag{28}$$

where k_2 and s_2 are positive constants.

Theorem 4.2: *For the underactuated ASV* (1)(2) *with the finite-time commander filtering* (16), *filtering error compensation mechanism* (23)(24) *and the heading control law* (28), *the heading steering task* $\psi = \psi_d$ *can be fulfilled in finite time.*

Proof: Consider the Lyapunov function candidate

$$V_2 = V_1 + \frac{1}{2}m_{33}{\varpi_2}^2 \tag{29}$$

Differentiating (29) yields

$$\dot{V}_2 = \varpi_1(\varpi_2 - k_1\varpi_1 - s_1|\varpi_1|^{\gamma}sign(\varpi_1) + \rho_1 sign(\zeta_1)) + \varpi_2(f_r + \tau_r + d_r - m_{33}\dot{\beta}_1 + k_2m_{33}\zeta_2 + m_{33}\zeta_1 + m_{33}\rho_2 sign(\zeta_2)) \tag{30}$$

Substituting (28) into (30) yields

$$\dot{V}_2 = m_{33}\varpi_1(\varpi_2 - k_1\varpi_1 - s_1|\varpi_1|^{\gamma}sign(\varpi_1) + \rho_1 sign(\zeta_1)) + \varpi_2(d_r - \hat{d}_r - m_{33}k_2\varpi_2 - m_{33}\varpi_1 - m_{33}s_2|\varpi_2|^{\gamma}sign(\varpi_2) + m_{33}\rho_2 sign(\zeta_2)) \tag{31}$$

Simplifying (31) yields

$$\begin{aligned}\dot{V}_2 =& -m_{33}k_1{\varpi_1}^2 - m_{33}k_2{\varpi_2}^2 - m_{33}s_1\varpi_1|\varpi_1|^{\gamma}sign(\varpi_1) - m_{33}s_2\varpi_2|\varpi_2|^{\gamma}sign(\varpi_2) + m_{33}\varpi_1\rho_1 sign(\zeta_1) + m_{33}\rho_2\varpi_2 sign(\zeta_2) + \varpi_2(d_r - \hat{d}_r)\\ \le& -\min\left\{2k_1 - \rho_1, 2k_2 - \rho_2 - \frac{1}{m_{33}}\right\} \times \left(\frac{m_{33}{\varpi_1}^2}{2} + \frac{m_{33}{\varpi_2}^2}{2}\right) + \frac{\rho_1 m_{33}sign^2(\zeta_1)}{2}\\ &- \min\left\{2s_1\left(\frac{1}{2}\right)^{\frac{1-\gamma}{2}}{m_{33}}^{\frac{1-\gamma}{2}}, 2s_2\left(\frac{1}{2}\right)^{\frac{1-\gamma}{2}}{m_{33}}^{\frac{1-\gamma}{2}}\right\} \times \left(\frac{m_{33}{\varpi_1}^2}{2} + \frac{m_{33}{\varpi_2}^2}{2}\right)^{\frac{\gamma+1}{2}}\\ &+ \frac{\rho_2 m_{33}sign^2(\zeta_2)}{2} + \frac{1}{2}(d_r - \hat{d}_r)^2\end{aligned} \tag{32}$$

then (32) is further derived as

$$\dot{V}_2 \le -\mu_1 V_2 - \mu_2 {V_2}^{\frac{\gamma+1}{2}} + K_1 \tag{33}$$

where

$$\mu_1 = \min\left\{2k_1 - \rho_1, 2k_2 - \rho_2 - \frac{1}{m_{33}}\right\}$$

$$\mu_2 = \min\left\{2s_1\left(\frac{1}{2}\right)^{\frac{1-\gamma}{2}}{m_{33}}^{\frac{1-\gamma}{2}}, 2s_2\left(\frac{1}{2}\right)^{\frac{1-\gamma}{2}}{m_{33}}^{\frac{1-\gamma}{2}}\right\}$$

$$K_1 = \frac{\rho_1 m_{33}sign^2(\zeta_1)}{2} + \frac{\rho_2 m_{33}sign^2(\zeta_2)}{2} + \frac{1}{2}(d_r - \hat{d}_r)^2$$

when $t \le t_d$,

$$e_r = d_r - \hat{d}_r = d_r - \int_0^t \mu_2 sign(\Pi_r)dt$$

$$\frac{\rho_1 m_{33}sign^2(\zeta_1)}{2} + \frac{\rho_2 m_{33}sign^2(\zeta_2)}{2} \le \frac{m_{33}\rho_1}{2} + \frac{m_{33}\rho_2}{2}$$

$$K_1 \le \frac{m_{33}\rho_1}{2} + \frac{m_{33}\rho_2}{2} + \Omega_1,$$

Since $sign(\Pi_r)$, d_r are bounded, then e_r is bounded. Besides, Ω_1 is a positive constant.

When $t > t_d$,

$$d_r - \hat{d}_r = 0$$

$$K_1 = \frac{\rho_1 m_{33}sign^2(\zeta_1)}{2} + \frac{\rho_2 m_{33}sign^2(\zeta_2)}{2} \le \frac{m_{33}\rho_1}{2} + \frac{m_{33}\rho_2}{2} = K_2$$

$$\dot{V}_2 \le -\mu_1 V_2 - \mu_2 {V_2}^{\frac{\gamma+1}{2}} + K_2,$$

The compensation tracking error ϖ_1 converges in finite time to

$$|\varpi_1| \le \max\left\{\sqrt{\frac{K_2}{\mu_1}}, \sqrt{2\left(\frac{K_2}{\mu_2}\right)^{\frac{2}{\gamma+1}}}\right\} \tag{34}$$

Suppose the Lyapunov function is chosen as.

$$V^* = \frac{1}{2}{\zeta_1}^2 + \frac{1}{2}{\zeta_2}^2 \tag{35}$$

Differentiating (35) yields:

$$\dot{V}^* = \zeta_1\dot{\zeta}_1 + \zeta_2\dot{\zeta}_2 = -k_1{\zeta_1}^2 - k_2{\zeta_2}^2 + \zeta_1(\beta_1 - \alpha) - \rho_1\zeta_1 sign(\zeta_1) - \rho_2\zeta_2 sign(\zeta_2)$$

Based on Lemma 4.1 and Lemma 4.2, we have $0 < |\beta - \alpha_0| \le \varrho_1$ in finite time.

$$\dot{V}^* \le -k_1{\zeta_1}^2 - k_2{\zeta_2}^2 + |\zeta_1||\beta_1 - \alpha| - \rho_1|\zeta_1|$$

$$
\begin{aligned}
&- \rho_2|\zeta_2| \\
&\le -k_1{\zeta_1}^2 - k_2{\zeta_2}^2 + (\varrho_1 - \rho_1)|\zeta_1| - \rho_2|\zeta_2| \\
&\le -\min\{2k_1, 2k_2\}\left(\frac{1}{2}{\zeta_1}^2 + \frac{1}{2}{\zeta_2}^2\right) \\
&\quad - \sqrt{2}\min\{\varrho_1 - \rho_1, \rho_2\} \\
&\quad \times \left(\frac{1}{2}{\zeta_1}^2 + \frac{1}{2}{\zeta_2}^2\right)^{\frac{1}{2}} \le -\mu_3 V^* - \mu_4 (V^*)^{\frac{1}{2}}
\end{aligned}
$$

where $\mu_3 = \min\{2k_1, 2k_2\}$, $\mu_4 = \sqrt{2}\min\{\varrho_1 - \rho_1, \rho_2\}$. Based on Lemma 4.3, V^* is finite-time stable, i.e. $\zeta_1 = \zeta_2 = 0$ in finite time $t^* = \frac{2}{\mu_3}\ln\left(\frac{\mu_3 (V^*)^{\frac{1}{2}} + \mu_4}{\mu_4}\right)$. Moreover, the finite-time stability of V_2 is guaranteed, ϖ_1 and $z_1 = \psi - \psi_d$ converge to zero in finite time. ■

4.3. Velocity control design

The desired velocity of ASV is assumed to be u_d, the control objective is to design the propulsion torque τ_u to make u converge to u_d in finite time. The velocity tracking error is defined as.

$$z_u = u - u_d \tag{36}$$

Choose the following integral terminal sliding mode

$$S_u = z_u - z_u(0) + c\int_0^t z_u^{\gamma_1} dt = 0 \tag{37}$$

where $c > 0$ and $0 < \gamma_1 < 1$.

Differentiating (37) yields

$$\dot{S}_u = \frac{m_{22}}{m_{11}} vr - \frac{d_{11}}{m_{11}} u + \frac{\tau_u}{m_{11}} + \frac{d_u}{m_{11}} - \dot{u}_d + c z_u^{\gamma_1} \tag{38}$$

To improve the convergence rate and dynamic response, a terminal reaching law is employed as

$$\dot{S}_u = -\varepsilon_1 S_u - \varepsilon_2 |S_u|^{\gamma_2} sign(S_u) \tag{39}$$

where $\varepsilon_1 > 0$, $\varepsilon_2 > 0$. The velocity tracking controller is designed as

$$
\begin{aligned}
\tau_u = m_{11}(&-\varepsilon_1 S_u - \varepsilon_2 |S_u|^{\gamma_2} sign(S_u) + \dot{u}_d - c z_u) \\
&- m_{22} vr + d_{11} u - \hat{d}_u
\end{aligned} \tag{40}
$$

Theorem 4.3: *For the underactuated ASV* (1)-(2) *with the integral terminal sliding mode* (37), *terminal reaching law* (39) *and the velocity tracking control law* (40), *the task* $u = u_d$ *can be fulfilled in finite time.*

Proof: Consider the Lyapunov function candidate

$$V_3 = \frac{1}{2}{S_u}^2 \tag{41}$$

Differentiating (41) and utilizing (40), we have

$$\dot{V}_3 = S_u \dot{S}_u$$

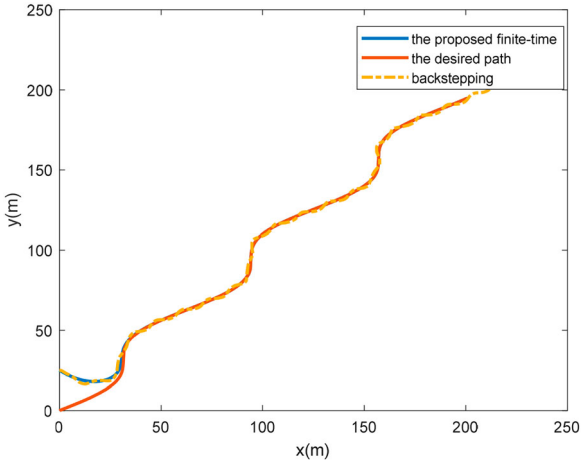

Figure 2. Path-following curve.

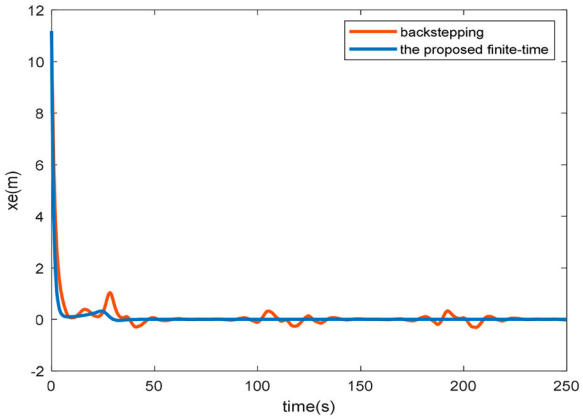

Figure 3. Position error along x-axis.

$$
\begin{aligned}
&= S_u\Big(-\varepsilon_1 S_u - \varepsilon_2 |S_u|^{\gamma_2} sign(S_u) \\
&\quad + \frac{1}{m_{11}}(d_u - \hat{d}_u)\Big) \\
&= -\varepsilon_1 {S_u}^2 - \varepsilon_2 S_u |S_u|^{\gamma_2} sign(S_u) + \frac{S_u}{m_{11}}(d_u - \hat{d}_u) \\
&\le -\min\left\{2\varepsilon_1, -\frac{1}{{m_{11}}^2}\right\}\left(\frac{{S_u}^2}{2}\right) \\
&\quad - 2\varepsilon_2\left(\frac{1}{2}\right)^{\frac{1-\gamma_2}{2}}\left(\frac{{S_u}^2}{2}\right)^{\frac{\gamma_2+1}{2}} \\
&\quad + \frac{1}{2}(d_u - \hat{d}_u)^2
\end{aligned}
$$

The above formula can be expressed as

$$\dot{V}_3 \le -\kappa_1 V_3 - \kappa_2 {V_3}^{\frac{\gamma_2+1}{2}} + \mathrm{K}_3$$

where $\kappa_1 = \min\left\{2\varepsilon_1, -\frac{1}{{m_{11}}^2}\right\}$, $\kappa_2 = 2\varepsilon_2\left(\frac{1}{2}\right)^{\frac{1-\gamma_2}{2}}$, $\mathrm{K}_3 = \frac{1}{2}(d_u - \hat{d}_u)^2$. When $t \le t_d$, $e_u = d_u - \hat{d}_u = d_u - \int_0^t \mu_2 sign(\Pi_u) d(t)$. Since $sign(\Pi_u)$ and d_u is bounded, then e_u is bounded and $\mathrm{K}_3 = \frac{1}{2}{e_u}^2 \le \Omega_2$, Ω_2 is a positive constant. V_3 converges to a specified compact set in $t \le t_d$. When $t > t_d$, $\mathrm{K}_3 = 0$, according to Lemma 4.3,

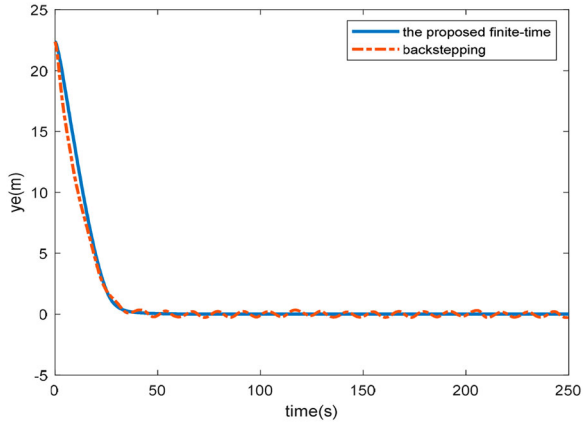

Figure 4. Position error along y-axis.

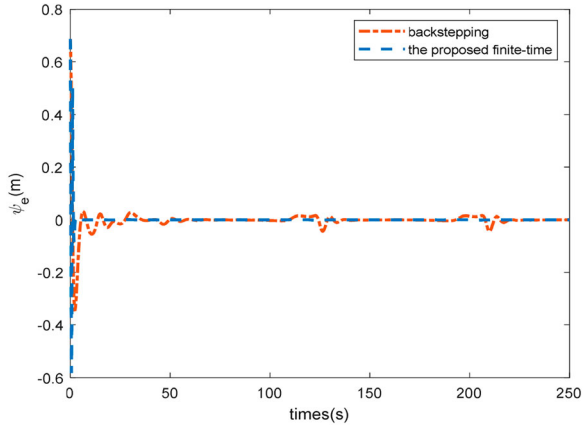

Figure 5. Heading position error.

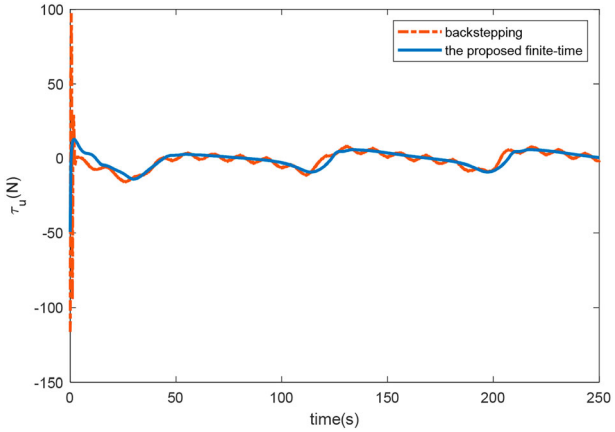

Figure 6. Longitudinal control.

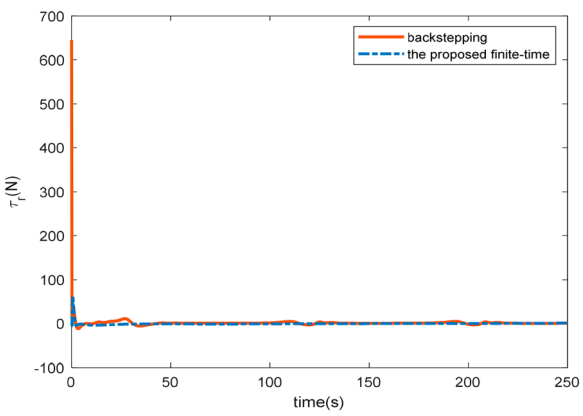

Figure 7. Yawing angular control.

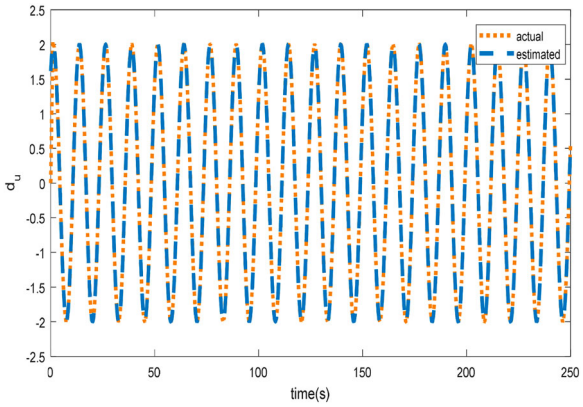

Figure 8. d_u estimation.

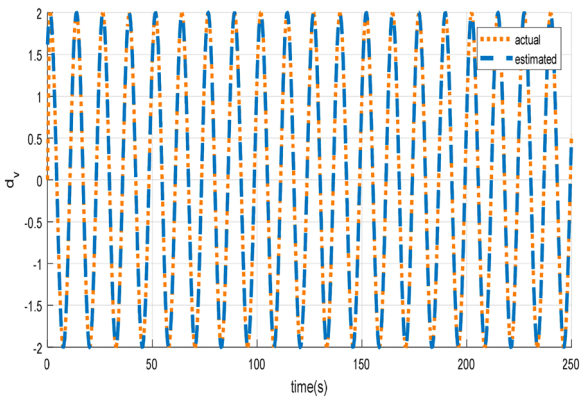

Figure 9. d_v estimation.

V_3 is finite-time stable. Then along the integral terminal sliding mode (37), $z_u = u - u_d$ converges to zero in finite time. ■

5. Simulation results

In order to verify the effectiveness and robustness of the proposed path-following controller, numerical simulations are carried out with a ASV model, whose parameters are $m_{11} = 25.8kg$, $m_{22} = 33.8kg$,$m_{33} = 2.76kg$; $d_{11} = 0.72kg/s$, $d_{22} = 0.86kg/s$, $d_{33} = 1.9kg/s$. A desired curve parametrized path is parameterized by $x_d = 10\sin(0.1\theta) + \theta$, $y_d = \theta$. The initial position of ASV is $[x(0), y(0), \psi(0)] = [0m, 25m, 0rad]$, the parameters of the disturbance observer and controller are $\mu_1 = 20$, $\mu_2 = 6$, $l_1 = 200$, $l_2 = 4000$, k_0 =1, $k_1 = 0.05$, $k_2 = 120$, $\rho_1 = \rho_2 = 10$, $c = 0.05$, $\varepsilon_1 = 2.5$, $\varepsilon_2 = 0.01$, $\Delta = 10$. Unknown disturbances in the external environment are $d_u = 2\sin(0.5t + 0.3\pi)$, $d_v = 2\cos(0.5t + 0.1\pi)$, $d_r = 2\cos(0.5t + 0.2\pi)$. The proposed control method is compared with the dynamic surface backstepping method by the same finite-time

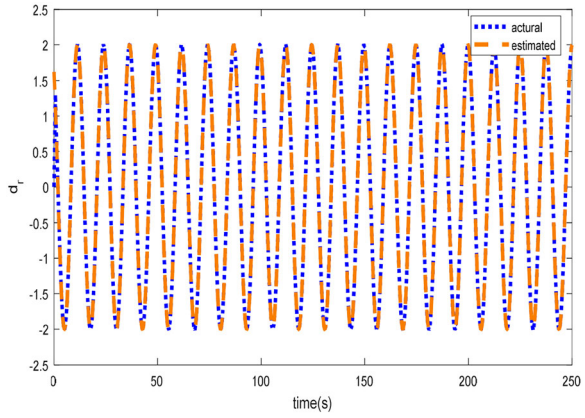

Figure 10. d_r estimation.

disturbance observer. The results show that the underactuated ASV moves along the desired path as shown in Figure 2, the path-following errors converge to zero in finite time as shown in Figures 3–5, and the better transient and steady performance is given with our proposed method. As observed in Figures 6–7, the proposed control inputs of the vehicle are more desirable with lower amplitude and smoother variation. Lastly, the estimated performance of the finite-time observer is shown in Figures 8–10, and the results demonstrate fast and accurate estimations of disturbances (d_u, d_v, d_r).

6. Conclusion

A finite-time control approach has been proposed for the kinematic path-following problem of the underactuated ASV exposed to disturbances. The LOS guide approach is utilized for the backstepping control framework with finite-time filter and finite-time disturbance observer. The differentiation explosion and control singularity problem with finite-time backstepping control is avoided. The theoretical analysis and simulation results show that faster convergence rate and higher tracking precision is achieved with the proposed scheme. Our further research work in this direction will focus on relaxing the assumption of the known bound of disturbance variation and extending it to fixed-time control and prescribed-time control.

Disclosure statement

No potential conflict of interest was reported by the author(s).

Funding

This work was supported by the Scientific Research Fund of Liaoning Provincial Education Department (LJKMZ20220737) and National Natural Science Foundatiion of China Foundation of China (62073054).

References

[1] Dai SL, He S, Lin H, et al. Platoon formation control with prescribed performance guarantees for USVs. IEEE Trans Ind Electron. 2017;65(5):4237–4246.

[2] Esfahani HN, Szłapczyński R. Model predictive supertwisting sliding mode control for an autonomous surface vehicle. Pol Marit Res. 2019;26:163–171. doi:10.2478/pomr-2019-0057

[3] Rasouli P, Shojaei K, Chatraei A. Output feedback look-ahead position control of electrically driven fast surface vessels. Automatika. 2016;57(4):968–981. doi:10.7305/automatika.2017.12.1485

[4] Peng Z, Wang J, Wang D. Distributed containment maneuvering of multiple marine vessels via neurodynamics-based output feedback. IEEE Trans Ind Eletron. 2017;64(5):3831–3839. doi:10.1109/TIE.2017.2652346

[5] Peng Z, Wang J, Wang D. Distributed maneuvering of autonomous surface vehicles based on neurodynamic optimization and fuzzy approximation. IEEE Trans Control Syst Technol. 2018;26(3):1083–1090. doi:10.1109/TCST.2017.2699167

[6] Zheng Z, Sun L, Xie L. Error-constrained LOS path following of a surface vessel with actuator saturation and faults. IEEE Trans Syst Man, Cybern Syst. 2018;48(10):1794–1805. doi:10.1109/TSMC.2017.2717850

[7] Fossen TI, Pettersen KY. On uniform semiglobal exponential stability (USGES) of proportional line-of-sight guidance laws. Automatica (Oxf). 2014;50(11):2912–2917. doi:10.1016/j.automatica.2014.10.018

[8] Jiang Y, Peng Z, Wang D, et al. Line-of-sight target enclosing of an underactuated autonomous surface vehicle with experiment results. IEEE Trans Ind Inform. 2020;16(2):832–841. doi:10.1109/TII.2019.2923664

[9] Huang Y, Wu D, Yin Z, et al. Design of UDE-based dynamic surface control for dynamic positioning of vessels with complex disturbances and input constraints. Ocean Eng. 2021;220:108487–37. doi:10.1016/j.oceaneng.2020.108487

[10] Hernández-Morales L, Valeriano-Medina Y, Hernández-Santana L, et al. Nonlinear guidance law algorithm applied to a small unmanned surface vehicle. Proc Inst Mech Eng, Part M: J Eng Maritime Environ. 2020;234(3):623–633.

[11] Souissi S, Boukattaya M, Damak T, et al. Adaptive control for fully-actuated autonomous surface vehicle with uncertain model and unknown ocean currents. Ocean Eng. 2020;217:108147–17. doi:10.1016/j.oceaneng.2020.108147

[12] Hu X, Wei X, Zhu G, et al. Adaptive synchronization for surface vessels with disturbances and saturated thruster dynamics. Ocean Eng. 2020;216:1–10.

[13] Hu C, Wang R, Yan F, et al. Robust path-following control for a fully actuated marine surface vessel with composite nonlinear feedback. Trans Inst Meas Control. 2018;40(12):3477–3488. doi:10.1177/0142331217727049

[14] Shen Z, Bi Y, Wang Y, et al. MLP neural network-based recursive sliding mode dynamic surface control for trajectory tracking of fully actuated surface vessel subject to unknown dynamics and input saturation. Neurocomputing. 2020;377:103–112. doi:10.1016/j.neucom.2019.08.090

[15] Lamraoui HC, Qidan Z. Path following control of fully actuated autonomous underwater vehicle based on

LADRC. Pol Marit Res. 2018;25(4):39–48. doi:10.2478/pomr-2018-0130

[16] Van M. Adaptive neural integral sliding-mode control for tracking control of fully actuated uncertain surface vessels. Int J Robust Nonlin Control. 2019;29(5):1537–1557. doi:10.1002/rnc.4455

[17] Liu S, Liu Y, Liang X, et al. Uncertainty observation-based adaptive succinct fuzzy-neuro dynamic surface control for trajectory tracking of fully actuated underwater vehicle system with input saturation. Nonlin Dyn. 2019;98(3):1683–1699. doi:10.1007/s11071-019-05279-w

[18] Zhao Z, He W, Ge SS. Adaptive neural network control of a fully actuated marine surface vessel with multiple output constraints. IEEE Trans Control Syst Technol. 2013;22(4):1536–1543.

[19] Wu W, Peng Z, Wang D, et al. Network-based line-of-sight path tracking of underactuated unmanned surface vehicles with experiment results. IEEE Trans Cybern. 2022;52(10):10937–10947. doi:10.1109/TCYB.2021.3074396

[20] Kong L, He W, Yang C, et al. Adaptive fuzzy control for a marine vessel with time-varying constraints. IET Control Theory Appl. 2018;12(10):1448–1455. doi:10.1049/iet-cta.2017.0757

[21] Wang N, Sun Z, Yin J, et al. Fuzzy unknown observer-based robust adaptive path following control of underactuated surface vehicles subject to multiple unknowns. Ocean Eng. 2019;176:57–64. doi:10.1016/j.oceaneng.2019.02.017

[22] Xu H, Oliveira P, Soares CG. L1 adaptive backstepping control for path-following of underactuated marine surface ships. Eur J Control. 2021;58:357–372. doi:10.1016/j.ejcon.2020.08.003

[23] Liu Z. Pre-filtered backstepping control for underactuated ship path following. Pol Marit Res. 2019;2:68–75. doi:10.2478/pomr-2019-0026

[24] Miao J, Wang S, Tomovic MM, et al. Compound line-of-sight nonlinear path following control of underactuated marine vehicles exposed to wind, waves, and ocean currents. Nonlin dyn. 2017;89:2441–2459. doi:10.1007/s11071-017-3596-9

[25] Xu B, Zhang L, Ji W. Improved non-singular fast terminal sliding mode control with disturbance observer for PMSM drives. IEEE T Transp Electr. 2021;7(4):2753–2762. doi:10.1109/TTE.2021.3083925

[26] Ghommam J, Iftekhar L, Saad M. Adaptive finite time path-following control of underactuated surface vehicle with collision avoidance. J Dyn Syst, Meas, Control. 2019;141(12):121–128. doi:10.1115/1.4044272

[27] Nie J, Lin X. FAILOS guidance law based adaptive fuzzy finite-time path following control for underactuated MSV. Ocean Eng. 2020;195:1–16.

[28] Zhu G, Ma Y, Hu S. Single-parameter-learning-based finite-time tracking control of underactuated MSVs under input saturation. Control Eng Pra. 2020;105:1–10.

[29] Levant A. Higher-order sliding modes, differentiation and output-feedback control. Int J Control. 2003;76(9-10):924–941. doi:10.1080/0020717031000099029

[30] Yu S, Yu X, Shirinzadeh B, et al. Continuous finite-time control for robotic manipulators with terminal sliding mode. Automatica (Oxf). 2005;41(11):1957–1964. doi:10.1016/j.automatica.2005.07.001

[31] Kang Z, Yu H, Li C. Variable-parameter double-power reaching law sliding mode control method. Automatika. 2020;61(3):345–351. doi:10.1080/00051144.2020.1757965